Available online at www.sciencedirect.com
ScienceDirect
Physica D 226 (2007) 11–22
PHYSICA D
www.elsevier.com/locate/physd

Heavy particles in incompressible flows: The large Stokes number asymptotics

Jérémie Bec[a,*], Massimo Cencini[b,c], Rafaela Hillerbrand[a,d]

[a] CNRS UMR 6202, Observatoire de la Côte d'Azur, BP4229, 06304 Nice Cedex 4, France
[b] CNR, Istituto dei Sistemi Complessi, Via dei Taurini 19, 00185 Roma, Italy
[c] INFM-SMC c/o Dip. di Fisica Università Roma 1, P.zzle A. Moro 2, 00185 Rome, Italy
[d] Institut für Theoretische Physik, Westfälische Wilhelms-Univ., Münster, Germany

Received 30 January 2006; received in revised form 21 June 2006; accepted 18 October 2006
Available online 12 December 2006
Communicated by A. Stuart

Abstract

The dynamics of very heavy particles suspended in incompressible flows is studied in the asymptotics in which their response time is much larger than any characteristic time of fluid motion. In this limit of very large Stokes numbers, particles behave as if suspended in a δ-correlated-in-time Gaussian flow. At those spatial scales where the fluid velocity field is smooth, following Piterbarg [L.I. Piterbarg, The top Lyapunov exponent for stochastic flow modeling the upper ocean turbulence, SIAM J. Appl. Math. 62 (2002) 777] and Mehlig et al. [B. Mehlig, M. Wilkinson, K. Duncan, T. Weber, M. Ljunggren, Aggregation of inertial particles in random flows, Phys. Rev. E 72 (2005) 051104], the two-particle dynamics is reduced to a nonlinear system of three stochastic differential equations with additive noise. This model is used to single out the mechanisms leading to the preferential concentration of particles. Scaling arguments are used to predict the large Stokes number behavior of the distribution of the stretching rate and of the probability distribution function of the longitudinal velocity difference between two particles. As for the fractal character of the particle distribution, strong numerical evidence is obtained in favor of saturation of the correlation dimension to the space dimension at large Stokes numbers. Numerical results at finite Stokes number values reveal that this model catches some important qualitative features of particle clustering observed in more realistic flows.

Keywords: Stochastic flows; Inertial particles; Lyapunov exponents; Preferential concentration

1. Introduction

Dust, impurities, droplets, air bubbles, and other finite-size particles transported by incompressible flows are commonly encountered in many natural phenomena and industrial processes. A salient feature of such suspensions is the presence of strong inhomogeneities in the spatial distribution of particles. This phenomenon is dubbed 'preferential concentration' (see, e.g., [1]). Such inhomogeneities affect the probability to find particles close to each other, and thus influence their possibility to collide or to interact biologically, chemically, or gravitationally. Examples showing the importance of the phenomenon are rain initiation by droplet coalescence in warm clouds [2] or planet formation by dust accretion in the solar system [3]. Engineering applications encompass optimization of spray combustion in diesel engines [4] and in rocket propellers [5].

Particles with a finite size and a mass density different from that of the carrier fluid have inertia. They do not evolve as simple point-like fluid tracers and are termed 'inertial particles'. It can be shown that if their size is below the smallest active scale of the flow (e.g. the Kolmogorov length scale in turbulent flows), the particles are subject to drag, buoyancy, added mass, etc. (see, e.g., [6]). Here we are interested in the limit where particles are not only very small, but also much denser than the surrounding fluid. They then interact with the fluid only through a Stokes viscous drag whose characteristic time (made dimensionless by normalizing it with the typical time scale of the carrier flow) is referred to as the 'Stokes number' *St*.

* Corresponding author.
E-mail address: bec@obs-nice.fr (J. Bec).

0167-2789/$ - see front matter © 2006 Elsevier B.V. All rights reserved.
doi:10.1016/j.physd.2006.10.007

Experiments [1,7] and numerics [8–10] show that the degree of inhomogeneity in the spatial distribution of the suspended particles is a non-trivial function of the Stokes number with a maximum at $St \approx 1$.

Quantifying analytically this dependence is an open question. Tools of dissipative dynamical systems are of great use for the investigation of those spatial scales on which the carrier flow is smooth. Indeed, in contrast to tracers in incompressible fluids, inertial particles dynamics is dissipative due to their friction with the fluid. In the position–velocity phase space, their trajectories converge to a dynamically evolving attracting set which is generically multifractal [11,12]. The particle spatial distribution, obtained by projecting this singular set onto the physical space, can also be multifractal [13]. Many observables introduced in the framework of dynamical systems, such as correlation dimension, Lyapunov exponents, or stretching rates, bring important information on particle concentration. Little is known about the dependence of these observables on the Stokes number. Several attempts in determining it have been made in simplified settings: small Stokes number asymptotics [14,15], Gaussian flows with finite [16–18,13] and zero correlation time [19,24,20–23].

In this paper we focus on inertial particles in the limit of very large Stokes numbers. In Section 2 we show that in this limit, no matter the actual nature of the underlying carrier flow provided it is statistically homogeneous and isotropic, the particles do behave as if suspended in a time-uncorrelated Gaussian flow. This result was derived independently in [25]. In Section 3, the approach of [19,21] is applied to write the relative motion of two suspended particles as a three-dimensional (random) dynamical system. This reduced dynamics is related to different observables quantifying inhomogeneities in the particle distribution. Some heuristic understanding of this model is provided.

In Section 4 we extend the scaling arguments developed in [23] to the large Stokes number behavior of velocity differences and of the stretching rate. Predictions are confirmed by numerical experiments which reveal algebraic tails with exponent -3 for the probability distribution function (pdf) of the longitudinal velocity difference between particles. A heuristic argument explaining this behavior is provided. The fractal (correlation) dimension is then investigated numerically in Section 5. Evidence is given that it saturates to the space dimension at sufficiently large values of the Stokes number.

Beside the physical relevance in the large St asymptotics, spatially smooth Gaussian carrier flows without time correlations are valuable models for systematic investigations. We thus study in Section 6 small and intermediate values of the Stokes number. In contrast to the quadratic behavior observed in more realistic flows [15,13,17], it is observed that for $St \ll 1$ the deviation from a uniform distribution is linear in St. However, the general qualitative picture is nonetheless in accordance with observations in real flows. In particular, simulations show that deviations from uniformity are strongest at intermediate values of the Stokes number. As a δ-correlated flow has no structure, this observation questions the phenomenological explanation of particle clustering often found in the literature (see, e.g., [1]). Section 7 is devoted to concluding remarks and summarizes the main findings. Appendix A provides some details on the numerical methods.

2. Model dynamics at large Stokes numbers

For suspensions that are so dilute that collisions, hydrodynamic interactions between particles and retro-action of the particles on the flow can be disregarded, the equations governing the evolution of a spherical particle with density ρ different from that of the carrier fluid ρ_f have been derived in [6]. It was assumed there that the particle radius a is much smaller than the Kolmogorov scale η and that the particle Reynolds number is very small. This implies that the flow surrounding the particle can be approximated by a pure Stokes flow.

In the present paper, we consider impurities that are much heavier than the carrier fluid ($\rho \gg \rho_f$) in the absence of gravity. The time evolution of the particle position $\boldsymbol{X}(t)$ then takes the simple form:

$$\frac{\mathrm{d}^2\boldsymbol{X}}{\mathrm{d}t^2} = -\frac{1}{\tau}\left[\frac{\mathrm{d}\boldsymbol{X}}{\mathrm{d}t} - \boldsymbol{u}(\boldsymbol{X}(t), t)\right], \tag{1}$$

where $\tau = (2\,a^2\,\rho)/(9\nu\rho_f)$ is the particle response time, the so-called 'Stokes time', and ν denotes the kinematic viscosity of the carrier fluid.

We are interested in particles with substantial inertia, meaning that $\tau \gg \tau_f$, where τ_f denotes the largest characteristic time of the carrier flow. In a first approximation, such particles relax so slowly to the fluid flow that, along their paths, the local structure of the fluid velocity field changes several times in the interval of time τ. Thus, on the typical time scales of particle motion, the effective fluid velocity field behaves as a time-uncorrelated process. This can be shown formally by rescaling the time as $s = t/\tau$, so that Eq. (1) becomes

$$\frac{\mathrm{d}^2\boldsymbol{X}}{\mathrm{d}s^2} = -\frac{\mathrm{d}\boldsymbol{X}}{\mathrm{d}s} + \tau\boldsymbol{u}(\boldsymbol{X}(\tau s), \tau s). \tag{2}$$

Now, the correlation time of the velocity field being finite and smaller than τ_f by definition of the latter, the central-limit theorem yields $\tau^{1/2}u_i(\boldsymbol{x}, \tau s) \overset{\text{law}}{\sim} \tilde{u}_i(\boldsymbol{x}, s)$ when $\tau \gg \tau_f$, where $\tilde{\boldsymbol{u}}$ is a δ-correlated Gaussian process and where the relation $\overset{\text{law}}{\sim}$ designates equivalence in probability law. With this expression and with transforming s back to the physical time t, (2) yields:

$$\frac{\mathrm{d}^2\boldsymbol{X}}{\mathrm{d}t^2} = -\frac{1}{\tau}\left[\frac{\mathrm{d}\boldsymbol{X}}{\mathrm{d}t} - \tilde{\boldsymbol{u}}(\boldsymbol{X}(t), t)\right]. \tag{3}$$

Hence, particles with very large inertia behave as if suspended in a Gaussian, δ-correlated in time carrier velocity field. For the sake of notation simplicity, we shall omit the tilde on the fluid velocity and refer to $\boldsymbol{u}$ as a δ-correlated carrier flow.

In many real flows, the small-scale properties can be understood by considering a spatially smooth, statistically homogeneous and isotropic velocity field. These spatial properties carry over to the limiting (Gaussian) process, whose

correlation $\langle u_i(\boldsymbol{x},t)\,u_j(\boldsymbol{y},t')\rangle = D_{ij}(\boldsymbol{x}-\boldsymbol{y})\,\delta(t-t')$, is thus given by

$$D_{ij}(\boldsymbol{r}) = 2D_0\,\delta_{ij} - d_{ij}(\boldsymbol{r}), \tag{4}$$

$$d_{ij}(\boldsymbol{r}) = D_1((d+1)r^2\,\delta_{ij} - 2\,r_i r_j) + o(r^2), \tag{5}$$

where $r = |\boldsymbol{r}|$ and d is the space dimension. The constants D_0 and D_1 measure the intensity of the velocity and of its gradient, respectively. They define two time scales of the velocity field. Considering particles with very large inertia implies that τ is much larger than these two time scales.

Note that the approximation of the fluid velocity by a δ-correlated noise has been rigorously derived for the first time in [24] in the case of Gaussian carrier flows. The case of turbulent flows has been considered recently with great detail in [25]. Such velocity fields with zero time correlation belong to the so-called 'Kraichnan ensemble' [26] and have been studied extensively in the last decade in passive scalar transport theory [27]. They are generally much more tractable than other random flows because of the Gaussianity and the δ-correlation in time. In particular, Eq. (3) together with (4) and (5) lead to closed equations for particle density correlations in the position–velocity phase space. In spite of such a simplification, a straightforward solution of these equations cannot be obtained with the standard techniques generally used in studying Fokker–Planck systems.

3. Two-particle dynamics

According to (3), the two-particle separation $\boldsymbol{R} = \boldsymbol{X}' - \boldsymbol{X}$ evolves as

$$\frac{\mathrm{d}^2\boldsymbol{R}}{\mathrm{d}t^2} = -\frac{1}{\tau}\left(\frac{\mathrm{d}\boldsymbol{R}}{\mathrm{d}t} - \delta\boldsymbol{u}\right), \tag{6}$$

where $\delta\boldsymbol{u} = \boldsymbol{u}\left(\boldsymbol{X}'(t),t\right) - \boldsymbol{u}\left(\boldsymbol{X}(t),t\right)$. For spatially smooth flows, the velocity difference $\delta\boldsymbol{u}$ can be approximated at small scales by $\boldsymbol{\sigma}(t)\,\boldsymbol{R}$, where $\sigma_{ij}(t) = (\partial u_i/\partial x_j)(\boldsymbol{X}(t),t)$ is the strain matrix along the trajectory $\boldsymbol{X}(t)$. In the asymptotics of $St \gg 1$, the velocity correlation functions are given by (4) and (5). Thus, $\boldsymbol{\sigma}$ is to leading order a Gaussian random matrix with correlation given by (see, e.g., [27]):

$$\langle\sigma_{ij}(t)\sigma_{kl}(t')\rangle = 2\delta(t-t') \times D_1[(d+1)\delta_{ik}\delta_{jl} - \delta_{ij}\delta_{kl} - \delta_{il}\delta_{jk}]. \tag{7}$$

The two-particle dynamics (6) can then be recast in terms of the following system of stochastic differential equations in the position–velocity phase space $(\boldsymbol{R},\boldsymbol{V})$:

$$\mathrm{d}\boldsymbol{R} = \boldsymbol{V}\,\mathrm{d}t,$$
$$\mathrm{d}\boldsymbol{V} = -\frac{1}{\tau}\boldsymbol{V}\,\mathrm{d}t + \frac{1}{\tau}\,\mathrm{d}\boldsymbol{\sigma}\,\boldsymbol{R}. \tag{8}$$

Here and henceforth we make use of the Ito formalism.

The two-point motion, given by (8) together with the correlation (7), depends on two time scales only: τ, the particle response time, and D_1^{-1}, the inverse of the typical velocity gradient (or equivalently the turnover time associated to the smallest length scale of the flow). Rescaling the physical time t by one of these two characteristic times, the resulting dynamics depends on a single non-dimensional parameter, the Stokes number $St \equiv D_1\tau$. In most real flows, D_1^{-1} is of the same order as the correlation time of the fluid flow. The asymptotics of large inertia hence requires us to consider $St \gg 1$. For turbulent carrier flows, both D_1^{-1} and the correlation time are typically proportional to τ_η, the eddy turnover time associated to the Kolmogorov scale η. The limit of large inertia thus implies that $St \simeq S_\eta = \tau/\tau_\eta \gg 1$, i.e. the Stokes number as it is normally defined in the literature is considered much larger than unity.

3.1. Reduced dynamics

In contrast to tracers, the dynamics of inertial particles has to be considered in the full $(2\times d)$-dimensional position–velocity phase space. However, in both two and three dimensions, the number of variables necessary to describe the relative motion of two particles can be reduced to three, namely the particle distance $R = |\boldsymbol{R}|$ and the velocity component $V_\parallel$ in the direction of $\boldsymbol{R}$ and $|\boldsymbol{V}_\perp|$ in the directions perpendicular to it. The relative velocity is thus decomposed as $\boldsymbol{V} = V_\parallel\hat{\boldsymbol{R}} + \boldsymbol{V}_\perp$ with $\hat{\boldsymbol{R}} = \boldsymbol{R}/|\boldsymbol{R}|$. This reduction was used in [19] and in [21] (see also [23]) for $d = 2$ and for $d = 3$ respectively. In terms of the non-dimensional velocity differences X and Y defined as

$$X \equiv \frac{\tau}{R}V_\parallel = \frac{\tau}{R^2}\boldsymbol{R}\cdot\boldsymbol{V} \quad\text{and}\quad Y \equiv \frac{\tau}{R}|\boldsymbol{V}_\perp| = \left|\frac{\tau}{R}\boldsymbol{V} - X\hat{\boldsymbol{R}}\right|$$

the original $(2\times d)$-dimensional dynamics (8) reduces for $d = 2$ to

$$\mathrm{d}R = XR\mathrm{d}s, \tag{9}$$

$$\mathrm{d}X = -\left(X + X^2 - Y^2\right)\,\mathrm{d}s + \sqrt{2St}\,\mathrm{d}B_1, \tag{10}$$

$$\mathrm{d}Y = -\left(Y + 2XY\right)\,\mathrm{d}s + \sqrt{6St}\,\mathrm{d}B_2. \tag{11}$$

Here the rescaled time is $s = t/\tau$ and the B_i's denote two independent Brownian motions. In $d = 3$ the equations for R and X are the same, while Y is a solution of

$$\mathrm{d}Y = -\left(Y + 2XY - \frac{4St}{Y}\right)\,\mathrm{d}s + \sqrt{6St}\,\mathrm{d}B_2. \tag{12}$$

In deriving these Langevin equations, one makes use of the specific form (7) for the correlation of the strain matrix $\boldsymbol{\sigma}$. Note that the positivity of Y has to be ensured by supplementing the system with reflective boundary conditions on the plane $Y = 0$.

While in the original system the noise depends on the particle relative distance R, it is now additive. However, the drift terms in the reduced system are nonlinear and differ in two and three dimensions. The term $\propto 1/Y$, which is present whenever $d \geq 3$, can be interpreted as a geometrical constraint on the reduced dynamics that prevents the velocity difference between the two particles from becoming exactly parallel to their separation (i.e. $Y = 0$). This occurs on a spatio-temporal set of co-dimension $d-1$. In two dimensions, an arbitrary vector that evolves in time generically intersects this set at discrete times. The geometrical constraint and hence the singular term are therefore absent.

Note that the difference between $d = 2$ and $d = 3$ is more apparent than substantial. Indeed, with the change of variables $\{X, Y\} \to \{X, \mathcal{Y} = Y^2\}$ both the two- and the three-dimensional case can be written as

$$\mathrm{d}X = -\left(X + X^2 - \mathcal{Y}\right) \mathrm{d}s + \sqrt{2St}\ \mathrm{d}B_1,$$

$$\mathrm{d}\mathcal{Y} = -2\left(\mathcal{Y} + 2X\mathcal{Y} - \alpha_d\, St\right) \mathrm{d}s + 2\sqrt{6St}\ \mathcal{Y}^{1/2}\mathrm{d}B_2,$$

where $\alpha_{d=2} = 3$ while $\alpha_{d=3} = 7$. This formulation involving a multiplicative noise term will not be used in the following as it is more convenient to work with the additive noise formulation (9)–(12).

3.2. Statistical characterization of two-point motion

As a consequence of (9), time integration of the non-dimensional longitudinal velocity difference X yields exponential growth of the inter-particle separation R in physical space:

$$R(s) = R(0)\ \exp\left(\int_0^s X(s')\,\mathrm{d}s'\right). \tag{13}$$

The Oseledets theorem ensures that, under the ergodicity hypothesis on the dynamics, the separation behaves as $R \propto \exp(\lambda t) = \exp(\lambda\tau s)$ at large times, λ being the important measure of particle relative motion. For instance, a positive Lyapunov exponent means that the particle dynamics is chaotic [11]. As shown in [19,21], a straightforward consequence of (13) is that the Lyapunov exponent can be expressed in terms of the reduced variables as

$$\lambda = \lim_{t\to\infty} \mu(t), \quad \text{where } \mu(t) = \frac{1}{t}\int_0^{t/\tau} X(s')\,\mathrm{d}s'. \tag{14}$$

If the reduced dynamics is ergodic (see discussion in the next subsection) one has $\lambda = \langle X\rangle/\tau$, where the angular brackets denote averages with respect to the realizations of the noises B_1 and B_2. At large but finite physical time t, the *stretching rate* $\mu(t)$ gets more and more sharply distributed around λ. More precisely, it obeys a large deviation principle and its pdf $p(\mu, t)$ takes the asymptotic form (see, e.g., [27,28])

$$\frac{\ln p(\mu, t)}{t} \sim -\frac{1}{\tau} H(\tau\mu) \quad \text{when } t \to \infty, \tag{15}$$

where H is a convex function attaining its minimum equal to 0 for $\mu = \lambda$. The *rate function* H measures the large fluctuations of μ, which are important to quantify particle clustering. Even if the Lyapunov exponent is positive, the finite-time stretching rate can be negative with a non-zero probability. This indicates that, although on average particles separate exponentially, they may spend a long time close to each other—a sign of a non-trivial clustering behavior.

The statistics of the stretching rate gives information on the *separation probability* $P_2(r)$, i.e. the probability that the distance R between two particles is less than r. This quantity is expected to behave as a power law at small distances:

$$P_2(r) \propto r^{\mathcal{D}_2} \quad \text{as } r \to 0. \tag{16}$$

The exponent $\mathcal{D}_2$ is usually referred to as the *correlation dimension* of the spatial distribution of particles [29,30]. When the particles distribute uniformly, $\mathcal{D}_2$ equals the space dimension d. Discrepancies from a uniform distribution appearing when $\mathcal{D}_2 < d$ are a signal of preferential concentration. The small-separation behavior (16) implies that the *generalized Lyapunov exponent* Λ of order $-\mathcal{D}_2$ vanishes (see, e.g., [28]), i.e.

$$\Lambda(-\mathcal{D}_2) \equiv \lim_{t\to\infty} \frac{1}{t} \ln\left\langle [R(t)/R(0)]^{-\mathcal{D}_2}\right\rangle = 0. \tag{17}$$

From (14), (15) and (17) one obtains that the correlation dimension is related to the rate function of the stretching rate through a Legendre transformation [27]: $\min_\rho\left[\mathcal{D}_2\,\rho + H(\rho)\right] = 0$.

Another useful quantity for characterizing inhomogeneous particle distributions is the *approaching rate* $\kappa(r)$. It is defined as the flux of particles that are separated by a distance less than r and approach each other, i.e. their longitudinal velocity difference $X(t)$ is negative:

$$\kappa(r) = \frac{1}{\tau}\left\langle RX\theta(-X)\,\theta(r - R)\right\rangle, \tag{18}$$

where θ denotes the Heaviside function. As discussed in [18], $\kappa(r)$ can be related to the binary collision rate in the framework of the so-called 'ghost collision scheme' [18,31]. This approach consists in counting collision events while allowing particles to overlap instead of scattering. At small separations the approaching rate behaves as a power law (see [18] for details):

$$\kappa(r) \propto r^{\gamma} \quad \text{as } r \to 0. \tag{19}$$

All the quantities introduced here, of course, depend on the only parameter of the dynamics, the Stokes number St. Their behavior in the limit $St \gg 1$ will be examined in Section 4 by means of scaling arguments applied to the reduced dynamics.

3.3. Qualitative picture

For two dimensions, the general picture of the drift in the (X, Y)-plane is shown in Fig. 1(a). Neglecting the effects of the gradient of the fluid velocity field (i.e. disregarding the noises in (10) and (11)), we are left with the drift term only. As shown in [19], the trajectories of the (X, Y)-plane are then circles passing by two fixed points. The unstable fixed point at $(-1, 0)$ corresponds to $V_\parallel = -R/\tau$, a relation between relative velocity and separation that is conserved by the dynamics. This relation leads to an exponential convergence of the trajectories of different particles to each other in physical space. The stable fixed point at $(0, 0)$ corresponds to a vanishing velocity difference and a constant spatial separation between the two particles. In this case, two particles have relaxed to the fluid motion and are then simply carried together by a uniform carrier flow with vanishing gradients. When the noise is neglected, this stable point attracts all trajectories except those located on the half-line $Y = 0$ with $X < -1$. The trajectories starting in the vicinity of this half-line perform very large circular loops before finally converging to the stable fixed point. Those starting exactly on the half-line escape to $X = -\infty$ in a finite time; their

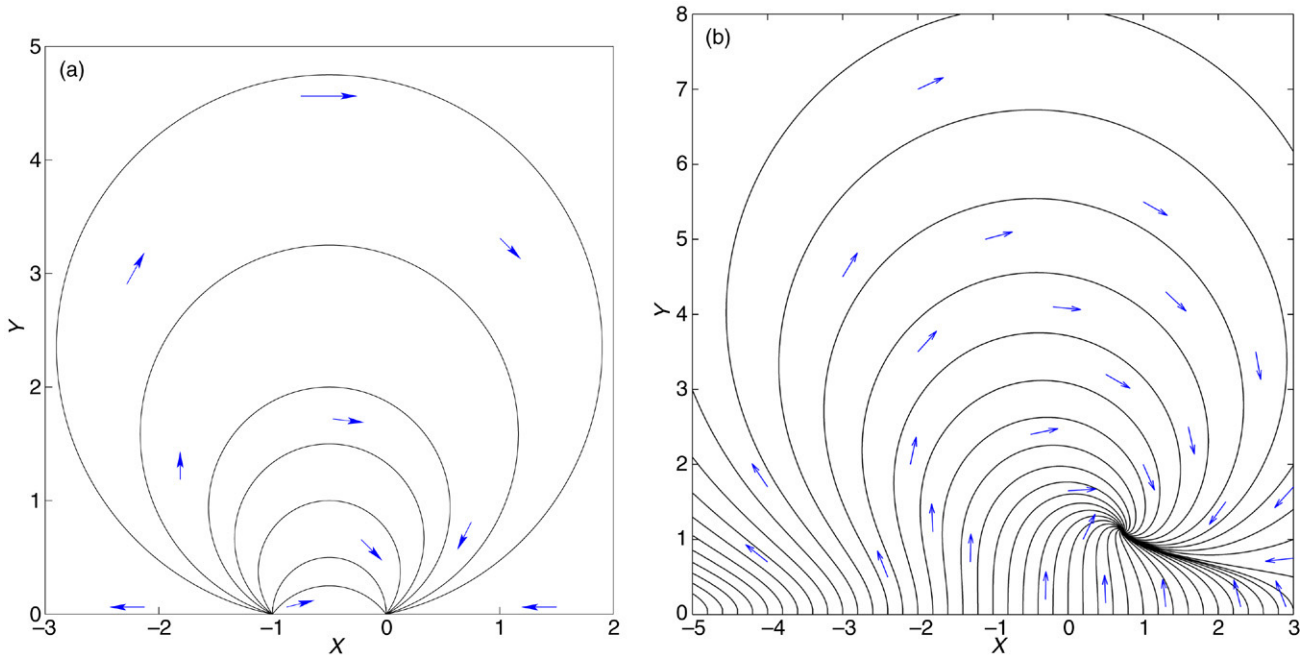

Fig. 1. Drift of the reduced system in the (X, Y)-plane for $d = 2$ (a) and $d = 3$ (b). X is the non-dimensional longitudinal velocity difference between two suspended particles; Y is the modulus of the non-dimensional velocity difference perpendicular to the particle separation.

longitudinal velocity difference is so large that the particles may cross each other within a finite time and their separation R vanishes in a time smaller than τ. Anyway, this happens with zero probability when noise is added. The presence of even a very small diffusion in the Y-direction prevents particles from remaining exactly on the $Y = 0$ line and thus from escaping to infinity.

In the presence of noise, particles spend a large fraction of time in the vicinity of the stable fixed point $(0, 0)$. There, both X and Y are very small, so that the dynamics of X and Y decouple and can be well approximated by two independent Ornstein–Uhlenbeck processes. When the noise contribution is sufficiently large, the trajectory can escape this linearized regime around the stable fixed point. In particular, the noise can push the trajectory to the left of the unstable fixed point with a small value of Y. There the drift acts as an accelerative term towards more negative values of X and finally dominates the diffusion. The trajectory then spends some time in the half-plane $(X < -1)$ before looping back to the positive-X half-plane when Y becomes sufficiently large. As we will see in Section 4.1, such events are responsible for power-law tails with exponent -3 in the pdf of X. Moreover, these loops provide a mechanism for bringing back to the right of the stable fixed point those trajectories that went away from its left. The presence of this flux implies that $\langle X \rangle > 0$. Although such events lead to a positive Lyapunov exponent $\lambda = \langle X \rangle / \tau > 0$, trajectories typically perform loops in the half-plane where $X < 0$ and thus the stretching rate μ, given by the time integral of X, can be very large negative. Note that during such events, the inter-particle distance R reaches very small values which is a signature of preferential concentration.

As stated in the previous subsection, mapping the reduced dynamics to the statistical properties of two-particle relative motion requires assuming that the former is ergodic. Even if such a property has been confirmed numerically, we have at the moment no rigorous proof of the fact that ensemble averages with respect to the velocity realizations can be replaced by time averages along particle trajectories. We however give a rather crude heuristic understanding why ergodicity can be reasonably assumed in two dimensions. The deterministic loops performed by the trajectories are completely determined by their stay in the neighborhood of the origin where the noise dominates. We expect this two-fold dynamics to provide a rapid loss of memory in the particle dynamics. Such mixing properties could ensure ergodicity of the dynamics.

For three dimensions, the general picture of the drift in the (X, Y) plane is given by Fig. 1(b). In contrast to the two-dimensional case, there is no unstable fixed point, but a unique stable fixed point that in the absence of noise attracts all trajectories. For sufficiently large values of the Stokes number, trajectories spiral towards the stable point, which is located in the first quadrant, at $X \approx Y \approx (2St)^{1/3}$ when $St \to \infty$. Like in two dimensions, the trajectories spend a large fraction of time in its neighborhood. They thus spend more time in the half-plane $(X > 0)$ than in the half-plane $(X < 0)$; this clearly implies that $\lambda = \langle X \rangle / \tau > 0$, so that the motion is expected to be chaotic in three dimensions as well. Unlike in two dimensions the line $Y = 0$ acts as a repeller. All trajectories starting there escape its vicinity with a transverse acceleration $\mathrm{d}Y/\mathrm{d}s \propto s^{1/2}$. They reach order unity values of Y in an algebraically fast time. Despite these differences, the mechanism leading to preferential concentration is essentially the same as for $d = 2$. In particular, the trajectories which after a strong fluctuation of the noise reach the half-plane $X < -1$ are accelerated to more negative values of X before looping back to the stable fixed point.

4. Scaling behavior in the asymptotics $St \to \infty$

The behavior of the statistical quantities related to the two-particle motion is investigated in this section for the limit for $St = D_1\tau \gg 1$. Following the scaling arguments developed in [23], we approach this limit by keeping $C = D_1/\tau^2$ constant. The limiting dynamics for $St \to \infty$ in two dimensions is then given by

$$\mathrm{d}\bar{X} = -\left(\bar{X}^2 - \bar{Y}^2\right)\mathrm{d}t + \sqrt{2C}\,\mathrm{d}B_1,$$
$$\mathrm{d}\bar{Y} = -2\,\bar{X}\bar{Y}\,\mathrm{d}t + \sqrt{6C}\,\mathrm{d}B_2, \qquad (20)$$

where t is the original physical time, $\bar{X} \equiv X/\tau$ and $\bar{Y} \equiv Y/\tau$. In three dimensions, the $\bar{Y}$ drift contains an additional term of the form $4C/\bar{Y}$. The scaling arguments presented in the following are valid in both two and three dimensions, and are confirmed by numerical experiments.

In order to obtain the scaling behavior of various quantities, we note that for $St \to \infty$ with C fixed, all statistical quantities can equivalently be derived from (10) and (11) or from (20). They only depend on the Stokes number in the former case and on the constant C in the latter. Assuming a smooth dependence on the two parameters, we derive closed differential equations for the quantities of interest. These equations yield the large St behavior of the observed quantities.

4.1. Probability distribution function of the longitudinal velocity

The pdf $p(x; St) = \langle\delta(x - X)\rangle$ of the non-dimensional longitudinal velocity difference X is related to the pdf $\bar{p}(\bar{x}; C)$ of $\bar{X}$ by

$$p(x; D_1\,\tau) = \frac{1}{\tau}\,\bar{p}\left(\frac{x}{\tau}; \frac{D_1}{\tau^2}\right),$$

where the factor $1/\tau$ is due to the Jacobian of the transformation from X to $\bar{X}$. The equality still holds when differentiating both sides with respect to D_1 or to τ. This allows us to write $\bar{p}(\bar{x}; C)$ as a solution of the partial differential equation

$$\bar{p} + \bar{x}\,\frac{\partial}{\partial\bar{x}}\,\bar{p} + 3C\,\frac{\partial}{\partial C}\,\bar{p} = 0,$$

which admits solutions that can be written $\bar{p}(\bar{x}; C) = C^{-1/3}q(C^{-1/3}\bar{x})$. Here q is an arbitrary differentiable function. The pdf of the longitudinal velocity difference can thus be written as

$$p(x; St) \approx St^{-1/3}q(St^{-1/3}x). \qquad (21)$$

Hence, at large Stokes numbers, the non-dimensional velocity difference X typically takes values of the order of $St^{1/3}$. The same argument can be applied for estimating the order of magnitude of the approaching rate κ defined in (18). This however does not give any information on the way κ depends on the particle distance r. Eq. (21) implies that the velocity difference $V = |\boldsymbol{V}|$ decreases as $D_1 St^{-2/3}$ when $St \to \infty$.

As seen from Fig. 2, simulations of the reduced dynamics in two dimensions (see Appendix A.1) for details on the numerical

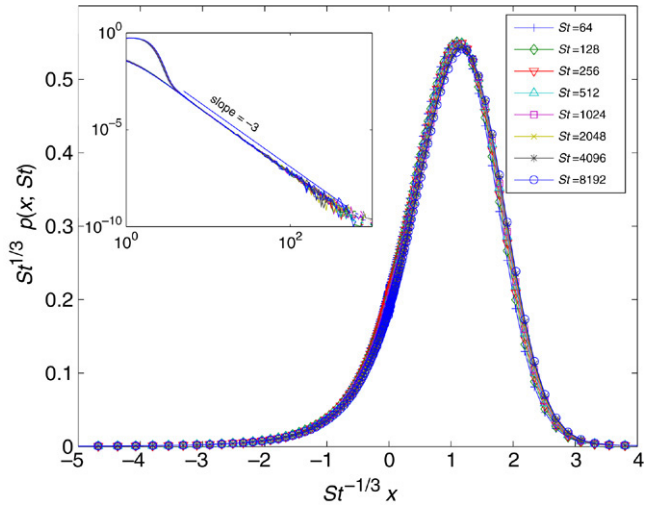

Fig. 2. Probability density function $p(x; St)$ of the non-dimensional longitudinal velocity difference X for various values of the Stokes number St in two dimensions. Inset: same in log–log coordinates.

method) show that the pdfs of X for different values of the Stokes number collapse. This confirms the scaling relation (21). The pdf of X has a peak for $x > 0$ which is a signature of the flux of probability from $x < 0$ to $x > 0$ induced by the loops of the (X, Y) trajectories described in the previous section.

The inset of Fig. 2 shows the distributions of X for several large values of St in log–log coordinates. The pdfs of the velocity difference display power-law tails with exponent -3 over two decades for both positive and negative values of X. This is again a signature of the very large loops characteristic of the dynamics in the (X, Y) plane. The observed power-law tails can be heuristically explained for large values of St by considering the limiting dynamics (20). Here the loops reaching large negative values of X are circles passing by $(0, 0)$. We now make a very crude approximation of the dynamics which is sketched in Fig. 3. When the trajectories are within a distance order unity of $(0, 0)$, the noise dominates and $\bar{X}$ and $\bar{Y}$ behave as two independent Brownian motions. At distances from the origin larger than unity, the drift dominates and the trajectories are circles. We turn to estimate the cumulative distribution function $P^<(x) = \mathrm{Prob}\,(\bar{X}(s) < x)$ for $x \ll -1$. Two separate contributions to $P^<$ have to be considered: (i) the probability to start a large loop that goes to the left-hand side of x and (ii) the fraction of time spent at $X < x$ during such a loop.

We first estimate contribution (i). To start a large loop that reaches values of $\bar{X}$ smaller than x, the trajectory must be at $\bar{X} \approx -1$ with $\bar{Y}$ sufficiently small. More precisely, the trajectory must be below the circle touching $\bar{X} = x$ when exiting the region where the noise dominates. This circle, which is represented by dots in Fig. 3, is defined by $\bar{X}^2 + (\bar{Y} + x)^2 = x^2$; for $\bar{X} = -1$ and x large, one has $\bar{Y} \propto (-x)^{-1}$. The probability to start a large loop is thus given by the probability that the two-dimensional Brownian motion (starting, for instance, at the origin) exits the circle of radius 1 from the infinitesimal interval $\bar{X} = -1$ and $0 \le \bar{Y} \le (-x)^{-1}$. This probability is clearly $\propto (-x)^{-1}$.

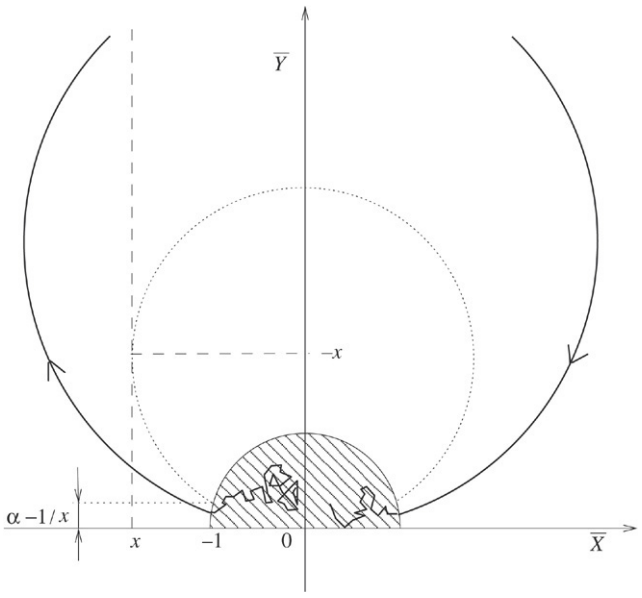

Fig. 3. Sketch of the simplified dynamics in the $(\bar{X}, \bar{Y})$ plane. A typical trajectory performing a large loop is represented as a bold line. At distances less than unity from the origin (striped area), the noise dominates and the trajectory is approximated by a pure Brownian motion. At larger distances, the drift dominates and the trajectories perform circular loops. In order to reach values of $\bar{X}$ smaller than $x \ll -1$, the trajectory must exit the striped area with $\bar{Y} = O(1/|x|)$.

We next estimate contribution (ii) that results from the fraction of time spent at $\bar{X} < x$ on a sufficiently large loop. It is easily checked from (20) that when neglecting noise and rescaling time by a factor $\propto R^{-1}$ the circular trajectories of radius R become circles with radius of order unity. This implies that the trajectories spend a time of order $(-x)^{-1}$ in the half-plane $\bar{X} < x$, whence a second contribution $\propto (-x)^{-1}$.

Lumped together, the two contributions (i) and (ii) imply that $P^{<}(x) \propto (-x)^{-2}$. Hence the pdf of the longitudinal velocity difference has a power-law tail with exponent -3 at large negative values. During the large loops, the trajectories in the $(\bar{X}, \bar{Y})$ plane also reach large positive values of $\bar{X}$ and of $\bar{Y}$. This gives again a fraction of time $\propto x^{-1}$ spent at both $\bar{X} > x \gg 1$ and $\bar{Y} > x \gg 1$. We hence have the same algebraic tail with exponent -3 for the pdf of both the longitudinal and the transversal velocity difference at large positive values.

This argument cannot be straightforwardly applied to the three-dimensional case. Firstly, the probability for the trajectories to enter a large loop cannot be estimated by linearizing the dynamics in the vicinity of the fixed point. Secondly, the numerical simulations of the reduced system are generally unstable for $d > 2$ (see Appendix A.2). At present, we do not know whether or not the power-law behavior $\propto |x|^{-3}$ for the pdf of X also holds in three dimensions.

4.2. The Lyapunov exponent and the stretching rate

As a direct consequence of (21), the Lyapunov exponent given by $\langle X \rangle / \tau$ behaves as

$$\lambda \approx \alpha\, C^{1/3} = \alpha\, D_1\, St^{-2/3}, \tag{22}$$

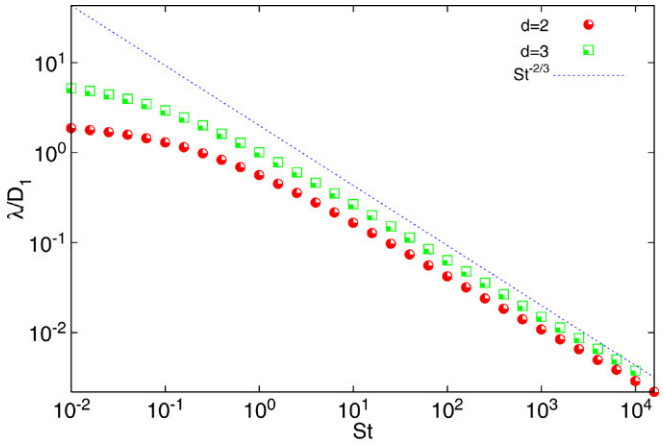

Fig. 4. Lyapunov exponent λ as a function of the Stokes number St in log–log coordinates in both two and three dimensions.

where $\alpha = \int \mathrm{d}z\, z q(z)$ is a constant. This result was obtained in [23] where it is shown that it holds even for compressible flows. Fig. 4 confirms numerically the power-law behavior (22) in both two and three dimensions. Note that the asymptotic regime is reached only for rather large values of St (typically larger than 100).

We now apply the scaling arguments of [23] to the rate function H of the large deviations of the stretching rate μ defined in (14). As for X, the asymptotic form for the pdf of μ given in (15) is equated with the pdf obtained from the system depending only on C. After differentiating this equation with respect to D_1 and τ, we obtain that $H(\rho = \tau\mu; St)$ obeys the following partial differential equation:

$$\rho \frac{\partial}{\partial \rho} H + 3\, St\, \frac{\partial}{\partial St} H = H.$$

From this relation the scaling form

$$H(\mu\tau; St) \approx St^{1/3} h\left(St^{-1/3}\mu\tau\right) \tag{23}$$

can be derived. This asymptotic behavior for the rate function of the large deviations of the stretching rate is confirmed by two-dimensional numerical experiments (see Fig. 5).

We have seen in the previous subsection that the Lyapunov exponent tends to zero as $St^{-2/3}$ in the limit $St \to \infty$. From the $St^{1/3}$ prefactor in the asymptotic form (23) and assuming, for instance, that H is a quadratic function, it is easily checked that the typical fluctuations of the stretching rate are $O(St^{-5/6})$. When $St \gg 1$ the stretching rate thus becomes more and more sharply distributed around the Lyapunov exponent, and, as expected, the dynamics indeed tends to be less and less intermittent.

5. Saturation of the correlation dimension

Particles with infinite inertia ($St = \infty$) need an infinite time for their velocity to relax to that of the fluid flow. In other terms they have a ballistic dynamics: they move freely maintaining their initial velocity. Hence such particles distribute uniformly in phase space [16]. The correlation dimension of their spatial distribution (defined in Section 3.2) equals the space dimension,

i.e. $\mathcal{D}_2 = d$. Furthermore, as the velocities of the particles become uncorrelated, the exponent γ characterizing the small-scale behavior of the approaching rate (see (19)) is expected to coincide with the correlation dimension. Thus, for $St \gg 1$ one has $\mathcal{D}_2 \simeq \gamma \simeq d$.

The scaling strategy devised in the previous section can only catch leading-order behavior of the correlation dimension, i.e. $\mathcal{D}_2 = d$. It hence cannot distinguish between the following two possible behaviors: (a) asymptotic convergence of $\mathcal{D}_2$ to d which is determined by subleading terms in the asymptotic form of H, and (b) saturation of $\mathcal{D}_2$ to d for Stokes numbers larger than a critical value $St^\dagger$. Based primarily on numerical analysis, we now present evidence for the latter.

Such a saturation can be understood by considering the particle motion in the full position–velocity phase space. As stated in the Introduction, the inertial particle dynamics is dissipative in phase space and the particle trajectories converge to a random attractor. This dynamically evolving set is typically characterized by a multifractal measure with a spectrum of dimensions $\overline{\mathcal{D}}_q$ [29,30,13]. In particular, the correlation dimension $\overline{\mathcal{D}}_2$ in phase space is the straightforward generalization of $\mathcal{D}_2$. It can be defined through the small-scale algebraic behavior of the probability $\overline{P}_2(r)$ to find two particles at a distance less than r in phase space:

$$\overline{P}_2(r) \sim r^{\overline{\mathcal{D}}_2} \quad \text{for } r \to 0.$$

To evaluate a distance in phase space we make use of the Euclidean norm $\sqrt{|\boldsymbol{R}|^2 + |\boldsymbol{V}/D_1|^2}$, where we choose to divide $\boldsymbol{V}$ by the typical gradient D_1 of the fluid flow in order to obtain a quantity with dimension of a length scale.

Clearly, particle positions are obtained by projecting from the $(2 \times d)$-dimensional phase space onto the d-dimensional physical space. It is then tempting to apply rigorous results that have been obtained on the projection of fractal sets [32,33]. In particular, it can be shown that for *almost all* projections, the correlation dimension of the projection of a random fractal set is the minimum of the correlation dimension of the object in the full space and of the dimension of the subspace onto which it is projected. In our case, this would lead to

$$\mathcal{D}_2 = \min\{d, \overline{\mathcal{D}}_2\}. \tag{24}$$

In the limit of large Stokes numbers, the particle motion becomes ballistic and thus $\overline{\mathcal{D}}_2 \to 2d$. This, together with the projection formula (24), suggests that there exists a critical value $St^\dagger$ of the Stokes number such that $\mathcal{D}_2(St) = d$ for all $St \geq St^\dagger$. However, determining whether $\mathcal{D}_2$ saturates above $St^\dagger$ or whether it approaches d asymptotically, depends on the genericity of the projection from phase space onto the physical space. Unfortunately, there is *a priori* no reason for assuming some kind of isotropy in phase space which would justify the validity of (24).

We are therefore led to investigating this issue numerically. A first idea was to estimate $\mathcal{D}_2$ and $\overline{\mathcal{D}}_2$ as the average local slopes of $P_2(r)$ and $\overline{P}_2(r)$, respectively. Such naive measurements lead to what is summarized in Fig. 6 that contradicts the projection formula (24). In particular, it is

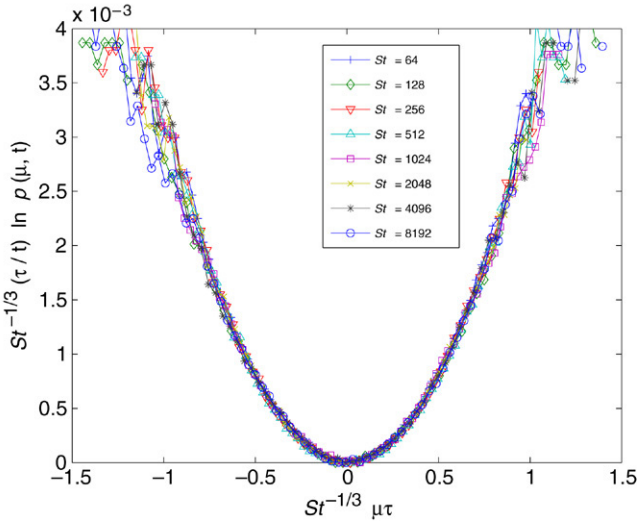

Fig. 5. Rate function of the stretching rate μ (or finite-time Lyapunov exponent).

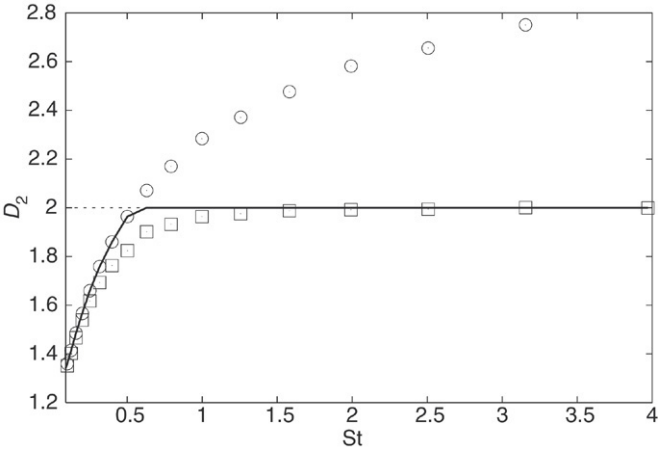

Fig. 6. Correlation dimension in physical space $\mathcal{D}_2$ (empty squares) and in phase space $\overline{\mathcal{D}}_2$ (empty circles) as a function of St. The solid curve represents the prediction based on the projection formula (24). The exponents were obtained by averaging the local slopes (logarithmic derivatives) of the pair separation probability. Errors in determining such exponents are of the order of the size of the symbol. See text and Fig. 7 for a discussion on the behavior of the local slopes.

observed that $\mathcal{D}_2 < \overline{\mathcal{D}}_2$ even when $\overline{\mathcal{D}}_2 < d$. The same kind of observation has been made in *ad hoc* examples where the projection is trivially typical, such as random fractal sets in three dimensions projected on randomly oriented planes [34]. This suggests we reconsider with more care the analysis of the data by performing a closer inspection of the local slopes (see Fig. 7(a) and (b)). One can naively estimate the dimensions by averaging the local slope over those scales where it seems fairly constant, thinking that the error on the exponent is of the order of the maximal deviations of the local slope from its mean. This method is appropriate for measuring $\overline{\mathcal{D}}_2$ but does not work for $\mathcal{D}_2$. Indeed, the logarithmic derivatives $(\mathrm{d}\ln P_2(r))/(\mathrm{d}\ln r)$ are curved, indicating a behavior that differs from a pure power law. This observation is made both below and above the potential critical Stokes number $St^\dagger \approx 0.6$ for which $\overline{\mathcal{D}}_2(St^\dagger) = d = 2$.

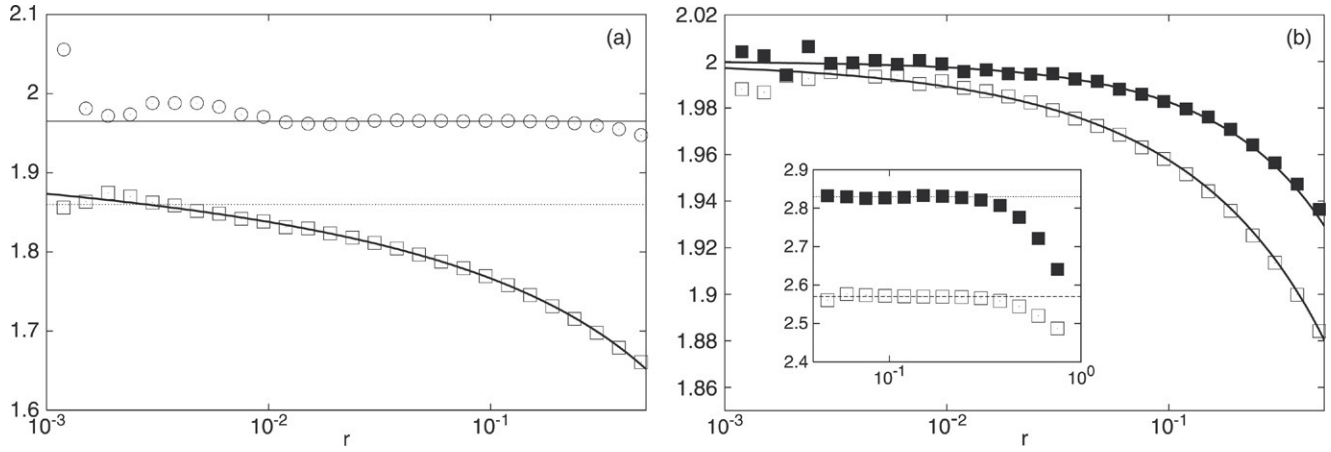

Fig. 7. (a) Logarithmic derivative $(\mathrm{d}\log P_2(r))/(\mathrm{d}\log r)$ of the pair distance probability in real space (empty boxes) and in phase space (empty circles) for $St = 0.5$. The solid straight line is at the estimated $\overline{\mathcal{D}}_2 = 1.965$, the dotted straight line is at the value 1.86 obtained by averaging the correlation dimension in real space in the range $[10^{-3} : 10^{-2}]$. The thick black line corresponds to a fit of the local slopes by assuming a superposition of two power laws, i.e. assuming $P_2(r) = Ar^a + Br^2$ (see text for a discussion). (b) Logarithmic derivative $(\mathrm{d}\log P_2(r))/(\mathrm{d}\log r)$ vs r for $St = 2.0$ (empty boxes) and $St = 4$ (full boxes). The curves are obtained by using (25) as a fitting function. The inset displays $(\mathrm{d}\log \overline{P}_2(r))/(\mathrm{d}\log r)$ vs r for $St = 2.0$ (empty boxes) and $St = 4$ (full boxes), for which $\overline{\mathcal{D}}_2 \approx 2.58$ and 2.83 respectively.

Similarly to what has been observed in other systems exhibiting multifractal behavior [35], one can be tempted to interpret the curvature of the local slopes by the presence of sub-dominant terms leading to the superposition of two power laws. We hence make the *Ansatz* that the probability distribution of the two-particle separation r can be approximated by $P_2(r) \simeq Ar^a + Br^b$ at the spatial scales we resolve. In our case it is rather clear how to guess the exponents a and b for $St < St^\dagger$. Since $\overline{\mathcal{D}}_2 < d$ in this range of Stokes numbers, one expects from (24) the projected set to have dimension $\mathcal{D}_2 = \overline{\mathcal{D}}_2$. However, at such values of St there is a contribution coming from caustics [36,18]. With a non-zero probability, particles can come sufficiently close to each other with quite different velocities. Once projected onto the physical space, these caustics will appear as spots of uncorrelated particles, and hence, locally, the correlation dimension will be $\mathcal{D}_2 = d = 2$. This (indeed very) crude argument suggests that

$$P_2(r) = Ar^{\overline{\mathcal{D}}_2} + Br^2. \tag{25}$$

As shown in Fig. 7, this fitting form is actually in very good agreement with the behavior of the local slopes. Indeed the validity of (25) was confirmed by several experiments which consisted in varying the number of free parameters in the fit. It is interesting to note that also for $St > St^\dagger$ the asymptotic form (25) approximates very well the data, even though the simple argument we sketched is not applicable for such values of the Stokes number.

To summarize, for St close to $St^\dagger$, the probability $P_2(r)$ is well approximated at small scales by the superposition of two power laws (25). The first power law gives the leading behavior for $St < St^\dagger$ and is related to the fractal nature of the particle distribution The second power law dominates for $St > St^\dagger$ and is related to the presence of caustics in the particle dynamics. We thus have strong evidence in favor of the validity of the projection formula (24) and hence for saturation of the correlation dimension $\mathcal{D}_2$ to the space dimension.

We now briefly comment upon the implication of saturation on the behavior of the approaching rate. In the limit $St \to \infty$, particles move ballistically and hence may approach each other within an arbitrary small distance with order unity velocity differences. One thus expects the exponent γ of the approaching rate defined in (19) to tend to d. As in the case of $\mathcal{D}_2$, deviations from this limiting value cannot be determined by scaling arguments. Saturation of $\mathcal{D}_2$ would however affect γ. It is related to a dominant contribution of caustics that could imply also the saturation of γ to d for sufficiently large Stokes numbers. As shown in the next section, though numerical experiments confirm this scenario, saturation cannot be studied with as much detail as for $\mathcal{D}_2$. In particular, there is at the moment no simple phenomenological argument leading to a prediction for the subleading terms.

6. The case of finite Stokes numbers

Apart from its validity for the large Stokes asymptotics, a Gaussian and δ-correlated in time carrier flow constitutes a valuable model for systematic investigation in particle clustering at any value of St: Due to the lack of persistent structures it is well suited for quantifying those effects in the particle dynamics that are due to its dissipative nature only.

Here we mostly stick to a numerical analysis whose main findings are summarized in Fig. 8: the correlation dimensions $\mathcal{D}_2$ and $\overline{\mathcal{D}}_2$ in physical space and in phase space, respectively, as well as the exponent γ characterizing the approaching rate, are represented as a function of the Stokes number.

The main feature is that for $St = St^\star \approx 0.07$, the correlation dimension has a minimum corresponding to a maximum of clustering. The presence of such an 'optimal' Stokes number $St^\star$ for particle clustering is a generic feature that has also been observed using other indicators, such as the deviation of the particle number density from a uniform distribution [1,9] or the Lyapunov dimension [37]. In turbulent flows, $St^\star$ was found to be of order of unity, i.e. the particle response time is of

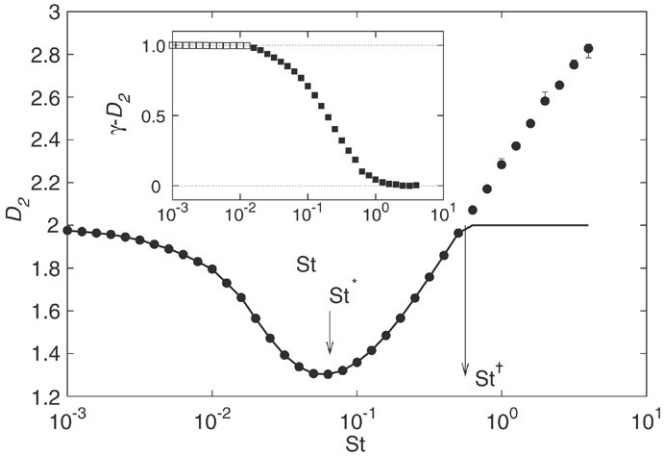

Fig. 8. Scaling exponents as a function of St. Data refer to the correlation dimension in real space $\mathcal{D}_2$ (thick solid line), which has been corrected for St close and larger than $St^\dagger$ using (24) and the correlation dimension in phase space $\overline{\mathcal{D}}_2$ (full circles). Inset: $\gamma - \mathcal{D}_2$ vs St. Note the plateaus at 1 for small St and at 0 for large St.

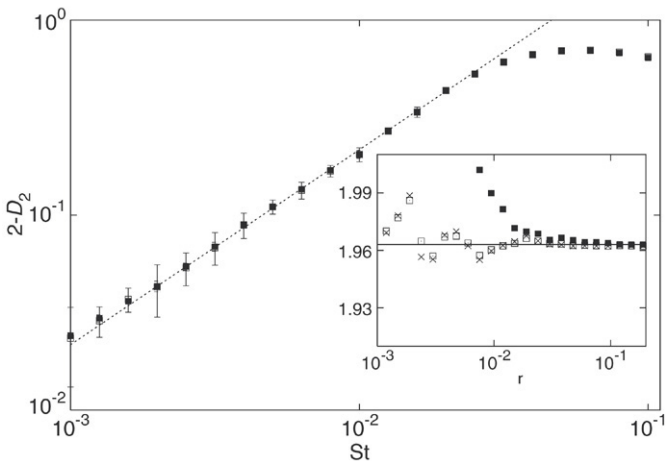

Fig. 9. Dimension deficits $2 - \mathcal{D}_2$ (empty boxes) and $2 - \overline{\mathcal{D}}_2$ (full boxes) as a function of St in log–log coordinates. Note the remarkable overlap that almost hides the empty boxes. The dashed straight line is the result of a linear fit $2 - \mathcal{D}_2 = 21.6St$. Inset: Logarithmic derivatives $(\mathrm{d}\log P_2(r))/(\mathrm{d}\log r)$ (empty boxes), $(\mathrm{d}\log \overline{P}_2(r))/(\mathrm{d}\log r)$ (full boxes), and $[(\mathrm{d}\log \kappa_2(r))/(\mathrm{d}\log r) - 1]$ (crosses) for $St = 1.6 \times 10^{-3}$, illustrating the typical quality of the scaling for $St \ll 1$.

the order of the Kolmogorov eddy turnover time. According to the standard phenomenological picture (see, e.g., [1]), this can be interpreted in terms of an optimal response time for the particles that anti-correlate with the vortical structures of the flow. This is responsible for the accumulation of particles in strain regions and, hence, for the formation of inhomogeneities in their spatial distribution. This appealing picture based on the presence of persistent structures in the fluid flow can, of course, not be applied to white-in-time random flows. Our results reveal that the mechanisms responsible for an optimal clustering have a purely dynamical origin. In our settings the only relevant time scale is D_1^{-1} which is a Lagrangian time scale (essentially the inverse of the Lyapunov exponent of fluid tracers). Even if we cannot exclude that time-correlated and time-uncorrelated flows are governed by different mechanisms, our conjecture is that particle clustering has a purely Lagrangian origin. A deeper understanding of such mechanisms is still lacking.

Qualitative agreement between the flow considered, which is uncorrelated in time, and more realistic flows displaying time correlations does not extend to $St \ll St^\star$. In the former, as seen from Fig. 9, the dimension deficit $2 - \mathcal{D}_2$ is proportional to St, while it was shown to be proportional to St^2 in both random time-correlated [17,13] and turbulent flows [15]. For $St \ll St^\dagger$, the scaling is rather clean and the subleading terms discussed in the previous section can hardly be detected and $\mathcal{D}_2 \approx \overline{\mathcal{D}}_2 \approx \gamma - 1$ (see insets of Figs. 8 and 9). These measurements suggest that in this regime the particle velocities are defining a smooth compressible velocity field. This leads us to conjecturing that the small Stokes number asymptotics can eventually be approximated with an expansion of the particle velocity as a function of the flow velocity. The validity of this expansion has been shown for correlated flows where it has been successfully used [38,14]. However this approach cannot be straightforwardly extended to the δ-correlated case where the fastest time scale of the system is the one of the fluid. Tackling this asymptotics requires the use of standard techniques of singular perturbation theories [39], which is beyond the scope of the present work.

The exponents characterizing the scaling of the approaching rate, as shown in the inset of Fig. 8, deviate from the small St asymptotics $\gamma = \mathcal{D}_2 + 1$ already for $St < St^\star$. They actually approach rapidly the large St asymptotics $\gamma \simeq \mathcal{D}_2$. This means that velocity differences of close particles become less and less correlated, i.e. $|\boldsymbol{V}| \sim |\boldsymbol{R}|^0$. Caustics seem to dominate the two-particle statistics already at intermediate values of the Stokes number.

We finally mention that we have performed similar numerical experiments in three dimensions. Although they involve fewer statistics, they reproduce qualitatively the same general picture.

7. Concluding remarks

We have seen that the fluid flow along particles with large inertia is asymptotic to a Gaussian, δ-correlated in time random process. We thus focused on two-particle motions in such an asymptotics. Following the approach of [19, 21], the dynamics of particle separation in position–velocity phase space has been reduced to three stochastic differential equations involving the distance, and the longitudinal and transverse velocity differences only. Focusing mostly on two dimensions, we reinterpreted within this approach many aspects of inertial particle dynamics such as, for instance, preferential concentration.

Scaling arguments have been used to determine the asymptotic behavior of the Lyapunov exponent, of the distribution of the stretching rate and of the velocity differences, predictions which are confirmed numerically. It would be of interest to test the validity of such scaling laws in time-correlated flows. Concerning the small-scale behavior of the spatial distribution of particles, we presented strong evidence

that the correlation dimension saturates to the spatial dimension when the Stokes number exceeds a threshold value $St^\dagger$. We extended our study to values of the Stokes number where the model loses its physical relevance, but is still displaying interesting features. For $St < St^\dagger$, we observed that particles transported by a δ-correlated flow reproduce the main qualitative features observed in more realistic time correlated flows. In particular, there exists an 'optimal' Stokes number St^* for particle clustering as observed for turbulent flows. Its existence in δ-correlated flows which have no structures, questions the classical phenomenological explanation based on the presence of persistent structures.

The probability distribution of the velocity difference between two particles was found to have power-law tails with exponent -3. We presented a phenomenological argument relating this algebraic behavior with those events where the particles approach each other ballistically. Interestingly, the correlation dimension of the particle distribution seems to depend analytically on the Stokes number and, in particular, it approaches linearly the space dimension d for $St \to 0$. This observation has to be balanced with results on the non-analyticity of the Lyapunov exponent for $St \to 0$ (see, e.g., [23] and references therein).

We conclude by stressing that a phenomenological understanding of the relative motion of inertial particles in turbulent flows may benefit from approaching the problem in terms of the reduced variables discussed here. In particular, studying the probability distribution of the components of the velocity difference might be of interest not only for checking whether or not the -3 tails are also present there, but to understand its behavior at finite Stokes numbers as well.

Acknowledgments

We are grateful to L. Biferale, A. Celani, G. Falkovich, A. Fouxon, U. Frisch, P. Horvai and S. Musacchio for useful discussions and remarks. Partial support by the EU under the research training network HPRN-CT-2002-00300 "Stirring and Mixing" is acknowledged. The stay of R.H. in Nice was supported by the Zeiss-Stiftung. M.C. acknowledges the Max Planck Institute for the Physics of Complex Systems for computational resources.

Appendix A. Numerical methods

With respect to numerics, efficient codes have been developed for the direct integration of the particle dynamics as it is given in (6) and of the reduced model dynamics (10) and (11).

A.1. Integration of the reduced model

In two dimensions, the exact solution of the drift part of the reduced model (10) and (11) can be straightforwardly derived from the solution of the deterministic part of (6). In terms of $Z = X + \mathrm{i}Y$, the solution can be cast into the following simple form [19]:

$$Z(t + \Delta t) = \frac{Z(t)\exp(-\Delta t)}{1 + Z(t)(1 - \exp(-\Delta t))}.$$

Then the noise term can be added by using the Euler–Ito scheme. This integration method is very efficient and has been used to evaluate the large deviations of the finite-time Lyapunov exponent and of the Lyapunov exponent itself.

In three dimensions, due to the Ito-term $\propto 1/Y$, the solution of the drift part cannot straightforwardly be obtained from the solution of the deterministic part of the original system as is done for $d = 2$. Due to the nonlinear terms in the drift, it is rather difficult to develop a stable integration scheme. We thus used the Lagrangian method described below.

A.2. Lagrangian integration of two-particle dynamics

The two-point motion (6) can be numerically integrated in a very efficient way by following [40]. In practice one simply needs to generate the random relative velocities according to a white-noise Gaussian process with a correlation function given by (4) and (5). This can be done easily because the correlation matrix d_{ij} in (5) is symmetric and positive definite. The latter property allows us to use the Cholesky decomposition of the correlation matrix,

$$d_{ij}(r) = L_{ik}L_{jk}.$$

L_{ij} being a non-singular lower triangular matrix. The integration of (6) can thus be performed with a standard Euler–Ito scheme

$$R_i(t + \Delta t) = R_i(t) + \Delta t V_i(t),$$
$$V_i(t + \Delta t) = \left(1 - \frac{\Delta t}{\tau}\right) V_i + \frac{1}{\tau}\sqrt{2\Delta t} L_{ij}\eta_j,$$

where $i, j = 1 \ldots d$, Δt is the discretized time step and the η_j's are d independent white noises.

The numerical procedure is thus as follows. Given the separation $\boldsymbol{R}$ between two particles, the correlation matrix $d_{ij}(r = |\boldsymbol{R}|)$ is computed from (5), and L_{ij} is obtained by means of an efficient algorithm. The d independent Gaussian variables η_j are generated and the velocity is obtained as $L_{ij}\eta_j$. In two spatial dimensions the latter procedure is particularly efficient. Indeed, the velocity differences associated to the particle separation $\boldsymbol{R} = (x, y)$ can be simply written as:

$$\delta u_x(t) = \sqrt{D_1}(x\eta_1 - y\eta_2)$$
$$\delta u_y(t) = \sqrt{D_1}(y\eta_1 + x\eta_1).$$

The evolution of the separation (6) is supplemented by periodic boundary conditions which are required for a stationary spatial particle distribution. These boundary conditions do not affect the small scales properties we are interested in.

This procedure has the advantage of working in a quasi-Lagrangian frame, i.e. directly with the particle relative position and the velocity difference. Furthermore, it can be easily generalized to rough flows. We used it for computing the pair-separation probability distribution, the phase–space correlation dimension and the approaching rate (see Section 6). The algorithm we set up is fast enough to allow us to reach statistics up to times of orders 10^8–10^9 (which for the smaller values of the Stokes number corresponds to 10^{13}–10^{14} time steps) in a few hours on a PC.

References

[1] J.K. Eaton, J.R. Fessler, Preferential concentrations of particles by turbulence, Int. J. Multiphase Flow 20 (1994) 169.

[2] R.A. Shaw, Particle-turbulence interactions in atmospheric clouds, Annu. Rev. Fluid Mech. 35 (2003) 183.

[3] I. dePater, J. Lissauer, Planetary Science, Cambridge University Press, Cambridge, 2001.

[4] S. Post, J. Abraham, Modeling the outcome of drop–drop collisions in Diesel sprays, Int. J. Multiphase Flow 28 (2002) 997.

[5] P. Villedieu, J. Hylkema, Modèles numériques lagrangiens pour la phase dispersée dans les propulseurs à poudre, Technical Report ONERA, March 2000.

[6] M.R. Maxey, J. Riley, Equation of motion of a small rigid sphere in a nonuniform flow, Phys. Fluids 26 (1983) 883.

[7] J.R. Fessler, J.D. Kulick, J.K. Eaton, Preferential concentration of heavy particles in a turbulent channel flow, Phys. Fluids 6 (1994) 3742.

[8] W.C. Reade, L.R. Collins, Effect of preferential concentration on turbulent collision rates, Phys. Fluids 12 (2000) 2530.

[9] K.D. Squires, J.K. Eaton, Preferential concentration of particles by turbulence, Phys. Fluids A 3 (1991) 1169.

[10] J. Bec, L. Biferale, G. Boffetta, A. Celani, M. Cencini, A. Lanotte, S. Musacchio, F. Toschi, Acceleration statistics of heavy particles in turbulence, J. Fluid Mech. 550 (2006) 349.

[11] J.-P. Eckmann, D. Ruelle, Ergodic theory of chaos and strange attractors, Rev. Modern Phys. 57 (1985) 617.

[12] L. Arnold, Random Dynamical Systems, in: Springer Monographs in Mathematics, Springer, Berlin, New York, 2003.

[13] J. Bec, Multifractal concentrations of inertial particles in smooth random flows, J. Fluid Mech. 528 (2005) 255.

[14] E. Balkovsky, G. Falkovich, A. Fouxon, Intermittent distribution of inertial particles in turbulent flows, Phys. Rev. Lett. 86 (2001) 2790.

[15] G. Falkovich, A. Pumir, Intermittent distribution of heavy particles in a turbulent flow, Phys. Fluids 16 (2004) L47.

[16] H. Sigurgeirsson, A.M. Stuart, A model for preferential concentration, Phys. Fluids 14 (2002) 4352.

[17] L.I. Zaichik, V. Alipchenkov, Pair dispersion and preferential concentration of particles in isotropic turbulence, Phys. Fluids 15 (2003) 1776.

[18] J. Bec, A. Celani, M. Cencini, S. Musacchio, Clustering and collisions of heavy particle in random smooth flows, Phys. Fluids 17 (2005) 073301.

[19] L.I. Piterbarg, The top Lyapunov exponent for stochastic flow modeling the upper ocean turbulence, SIAM J. Appl. Math. 62 (2002) 777.

[20] B. Mehlig, M. Wilkinson, Coagulation by random velocity fields as a Kramers problem, Phys. Rev. Lett. 92 (2004) 250602.

[21] B. Mehlig, M. Wilkinson, K. Duncan, T. Weber, M. Ljunggren, Aggregation of inertial particles in random flows, Phys. Rev. E 72 (2005) 051104.

[22] K. Duncan, B. Mehlig, S. Östlund, M. Wilkinson, Clustering by mixing flows, Phys. Rev. Lett. 95 (2005) 240602.

[23] P. Horvai, Lyapunov exponent for inertial particles in the 2D Kraichnan mode as a problem Anderson localization with complex valued potential, preprint nlin.CD/0511023.

[24] G. Pavliotis, A. Stuart, White noise limit for inertial particles in a random field, Multiscale Model. Simul. 1 (2003) 527.

[25] A. Fouxon, P. Horvai, Lyapunov exponent for inertial particles in developed turbulence (in preparation).

[26] R.H. Kraichnan, Small-scale structure of a scalar field convected by turbulence, Phys. Fluids 11 (1968) 945.

[27] G. Falkovich, K. Gawędzki, M. Vergassola, Particles and fields in fluid turbulence, Rev. Modern Phys. 73 (2001) 913.

[28] G. Paladin, A. Vulpiani, Anomalous scaling laws in multifractal objects, Phys. Rep. 156 (1987) 147.

[29] P. Grassberger, Generalized dimensions of strange attractors, Phys. Lett. A 97 (1983) 227.

[30] H.G.E. Hentschel, I. Procaccia, The infinite number of generalized dimensions of fractals and strange attractors, Physica D 8 (1983) 435.

[31] L.-P. Wang, A.S. Wexler, Y. Zhou, On the collision rate of small particles in isotropic turbulence. Part I. Zero-inertia case, Phys. Fluids 10 (1998) 266.

[32] T.D. Sauer, J.A. Yorke, Are the dimensions of a set and its image equal under typical smooth functions? Ergodic Theory Dynam. Systems 17 (1997) 941–956.

[33] B. Hunt, V. Kaloshin, How projections affect the dimension spectrum of fractal measures, Nonlinearity 10 (1997) 1031.

[34] N. Sánchez, E.J. Alfaro, E. Pérez, The fractal dimension of projected clouds, Astrophys. J. 625 (2005) 849–856.

[35] L. Biferale, M. Cencini, A. Lanotte, M. Sbragaglia, F. Toschi, Anomalous scaling and universality in hydrodynamic systems with power-law forcing, New J. Phys. 6 (2004) 37;
D. Mitra, J. Bec, R. Pandit, U. Frisch, Is multiscaling an artifact in the stochastically forced Burgers equation? Phys. Rev. Lett. 94 (2005) 194501.

[36] M. Wilkinson, B. Mehlig, Caustics in turbulent aerosols, Europhys. Lett. 71 (2005) 186.

[37] J. Bec, Fractal clustering of inertial particles in random flows, Phys. Fluids 15 (2003) L81.

[38] M.R. Maxey, The gravitational settling of aerosol particles in homogeneous turbulence and random flow fields, J. Fluid Mech. 174 (1987) 441.

[39] G. Papanicolaou, Some probabilistic problems and methods in singular perturbations, Rocky Mountain J. Math. 6 (1976) 653–673.

[40] U. Frisch, A. Mazzino, A. Noullez, M. Vergassola, Lagrangian method for multiple correlations in passive scalar advection, Phys. Fluids 11 (1999) 2178.